Geology, Geophysics & Environment 2024, vol. 50 (4): 421–442

Arsenic in water from the Bystre Thrust-Sheet (Outer Carpathians, Poland): Geological and environmental implications

Urszula Aleksander-Kwaterczak[1], Jakub Andrzejak[2], Anna Świerczewska[3], Konrad Lukaj[4]

[1] *AGH University of Krakow, Faculty of Geology, Geophysics and Environmental Protection, Krakow, Poland, e-mail: aleksa@agh.edu.pl (corresponding author), ORCID ID: 0000-0002-2932-3589*
[2] *ORCID ID: 0009-0000-0844-3082*
[3] *AGH University of Krakow, Faculty of Geology, Geophysics and Environmental Protection, Krakow, Poland, ORCID ID: 0000-0003-3464-6419*
[4] *ORCID ID: 0009-0007-2338-1722*

Received: 17 June 2024; accepted: 8 December 2024; first published online: 27 December 2024

Abstract: The article focuses on the physicochemical parameters of water in streams, springs, boreholes, and intakes from the Bystre Thrust-Sheet (the Silesian Nappe, Fore-Dukla Zone), the only area in the Polish segment of the Outer Carpathians where arsenic minerals occur. These waters are characterized by the presence of arsenic, lithium, mercury, barium, strontium and usually high CO_2 concentrations. The study aimed to determine the range of the geochemical anomaly of arsenic in water. An important aspect was to determine the origin of As and link its presence with the content of ions of other chemical elements dissolved in water. The sampling points were designated based on geological maps with a particular emphasis on the occurrence of tectonic dislocations and the configuration of the river network. In the selected places 47 samples of water were taken, and various elements were determined. Then, the range of occurrence of various types of water that differed from the average concentrations of selected ions was analysed. The potential relationship between the chemical composition of water and the geology of the Bystre Thrust-Sheet was also discussed. The high concentrations of arsenic were found only in springs and boreholes. In flowing waters, these concentrations quickly decreased as due to dilution or precipitation and binding with the solid phase. Relatively high (max. 378.72 μg/L) arsenic concentration, which significantly exceeded the permissible value (50 μg/L), was detected in the Bystre 1 borehole. This water has a pH value of 7.85 indicating its alkaline nature. When considering water use for health purposes, it is necessary to monitor its arsenic content. The conditions prevailing in waters, mainly high pH, favour the immobilization of metals in sediments and suspended matter. The lower concentrations of arsenic in flowing waters may be attributed to the strongly calcareous nature of the Cieszyn beds which act as a natural barrier, limiting the migration of arsenic beyond the Bystre Thrust-Sheet.

Keywords: Polish Outer Carpathians, the Bystre Thrust-Sheet, arsenic, watercourses, geochemical anomalies, geological structure

INTRODUCTION

The work intends to explain the potential geological sources of the presence of arsenic in the aquatic environment and to identify the extent of the geochemical anomaly of this metalloid in waters. Additionally, the chemical composition of water in the area where the arsenic anomaly occurred was examined, making it possible to link the occurrence of arsenic compounds with other water

components and the geological structure. The results have practical significance for assessing water quality and determining its suitability for human consumption. This is important information because the Bystre Thrust-Sheet region is considered a health resort area.

Arsenic in the environment

Arsenic is an element that occurs naturally in the earth's crust and is widely distributed throughout many components of the environment but mainly in rocks, soils, sediments and waters. It can migrate and transform as a result of volcanic eruptions, weathering, and the breakdown of organic matter. Human activity will also contribute to this, mainly through mining, the burning of fossil fuels, pesticide use, and employment in industry, primarily as an alloying agent in the production of pigments, textiles, paper, wood preservatives, and in the hide tanning process (Smedley & Kinniburgh 2002).

The chemical processes causing the formation of arsenic in the environment are complex and depend on many factors (De & Roy 2023). The mobility of this element in the environment depends largely on its oxidation state, pH as well as the presence of Fe(III), Al(III), or Mn(III/IV) (hydr)oxides, clay minerals, and humic substances which can adsorb arsenic compounds (Bissen & Frimmel 2003). It can be found in the environment in several oxidation states but in the natural aquatic environment, it occurs mainly in inorganic form as oxygen anions of arsenite – As(III), or arsenate – As(V). Arsenite which is found in reducing environments, mainly in sediments and groundwater, is mobile and toxic, while arsenate is more common in oxidizing environments, such as surface water, and is more stable, and therefore less bioavailable (Rahman et al. 2009). Among the organic forms, methylated As species are particularly common, but typically occur at much lower concentrations in water than inorganic forms of As (Campbell & Nordstrom 2014).

Arsenic is a specific metalloid. It is mobile at pH values of 6.5–8.5 and over various redox conditions under both oxidizing and reducing. However, in acidic environments, As tends to be more mobile and bioavailable (Ravenscroft et al. 2009). Arsenic can occur in waters as dissolved arsenic sulphides if the water is rich in reduced sulphur. Reducing and simultaneously acidic conditions favour the precipitation of realgar (AsS), orpiment (As_2S_3) or other sulphide minerals containing co-precipitated As. Therefore, if there is a high concentration of free sulphide in waters, high As contents can rarely be expected (Moore et al. 1988, Cullen & Reimer 1989, Bowell et al. 2014).

Arsenic occurs in the environment in a variety of chemical forms and mineral phases and is a major constituent in more than 200 minerals, including elemental As, oxides, sulphides, arsenides, arsenates and arsenites. The most abundant As ore mineral is arsenopyrite (FeAsS – up to 46 wt.% As), and the less common ones, but rich in arsenic, include realgar (AsS – up to 70 wt.% As) and orpiment (As_2S_3 – up to 61% weight As). Generally, arsenopyrite and the other dominant As-sulphide minerals are formed under high-temperature conditions in the earth's crust (Smedley & Kinniburgh 2002). Authigenic arsenopyrite is also formed in low-temperature sedimentary environments under reducing conditions (Bowell et al. 2014, Jarmołowicz-Szulc et al. 2024) and orpiment can be formed by microbial precipitation (Newman et al. 1998). A study of microbial organisms in wetland soils (Drahota et al. 2017) showed that realgar deposits can be also formed in strictly anaerobic organic-rich domains dominated by sulphate-reducing and fermenting metabolisms. Arsenic, as arsenopyrite (FeAsS) or as pyrite's (FeS_2) impurities (Assis et al. 2012), as well as realgar and orpiment (Nieć et al. 2016) is also quite often associated with gold mineralization.

Long-term exposure to inorganic arsenic, mainly through drinking water and food, can lead to chronic arsenic poisoning results with a plethora of dermatological and non-dermatological health effects including multi-organ cancer and early mortality (Bhattacharjee et al. 2013). Dangerously high levels of arsenic have been found in groundwater in more than 70 countries, including the likes of India, Canada, the United States of America, Australia, Taiwan, Mexico, Mongolia, Argentina, Chile, and Bangladesh (e.g. Uddin et al. 2006, Argos et al. 2010, Hubaux et al. 2012).

Geological setting

The study area is located in the eastern part of the Polish segment of the Outer Carpathians, in the Bieszczady Mountains. The fieldwork was carried out in the Bystre Thrust-Sheet (the Bystre Slice, Ślączka 1958), located in the Fore-Dukla Zone (Świdziński 1958) called also Fore Dukla Thrust-Sheet (Oszczypko et al. 2008). The Bystre Thrust-Sheet is a south-verging tectonic structure consisting of a system of several thrust slices (Rubinkiewicz 1998, 2007).

The strongly tectonically deformed Fore-Dukla Zone constitutes the southernmost part of the Silesian Nappe, one of the nappes of the Outer Carpathians. It borders the Central Carpathian Depression of the Silesian Nappe to the north and the Dukla Nappe overthrust to the south (Oszczypko et al. 2008). In this part of the Carpathians, the Silesian Nappe is formed by Cretaceous-Miocene marine sedimentary rocks (e.g. Jankowski & Ślączka 2014). The flysch sandstone, shales and marls of the Bystre Thrust-Sheet belong to seven lithostratigraphic units, ranging in age from the Early Cretaceous to the Eocene (Ślączka 1958, Jankowski & Ślączka 2000). Listing them from the oldest to the youngest, there are the Lower Cretaceous Cieszyn, Grodziszcze, Lgota, and Godula beds, the Upper Cretaceous-Paleocene Istebna beds, and the Eocene Hieroglyphic beds. Jarmołowicz-Szulc et al. (2024) believe that Oligocene Menilite beds occur near the southern boundary of the Bystre Thrust-Sheet. Intense tectonic deformations cause stratigraphic sections to be discontinuous.

The Bystre Thrust-Sheet is an area where calcite and quartz mineralization as well as bituminous impregnations commonly occur (e.g. Rybak 2000, Jarmołowicz-Szulc et al. 2012). The observed strong silicification of the Istebna sandstones is atypical for flysch formations (Peszat et al. 1985). In the stream sections, calcareous sinter is commonly observed especially in the vicinity of the brittle deformation zones.

The metallic mineralization is also noted. Two types have been distinguished: primary and epigenetic (Rybak 2000, Jarmołowicz-Szulc et al. 2023, 2024). Pyrite, galena, marcasite and sphalerite belong to the primary mineralization and there is no connection between such mineralization and the tectonics of the Bystre Thrust-Sheet (Rybak 2000). Epigenetic mineralization is associated with dislocated zones, with minerals such as quartz, realgar, orpiment and cinnabar (Rybak 2000, Jarmołowicz-Szulc et al. 2023, 2024).

The occurrence of minerals containing arsenic in the Bystre Thrust-Sheet was first recorded by Kamieński (1937) and studied in detail thanks to deep drilling holes and mining excavations in this area (Ostrowicki 1958, Ślączka 1958, Kita-Badak 1970, Nieć et al. 2016). Realgar was found in the Lgota and Istebna beds (Rybak 2000). It occurs there in veins, lenses, and/or impregnations in tectonic deformation zones and breccias. According to Jarmołowicz-Szulc et al. (2024), this mineral also occurs in the Menilite beds. The width of the mineralized zone can reach up to 60 m (Kita-Badak 1970). The realgar mineralization is characteristic only for this part of the Carpathians in Poland (Rybak 2000). Realgar is accompanied by orpiment in minor amounts (Nieć et al. 2016, Jarmołowicz-Szulc et al. 2024). At the exposures, it is visible almost exclusively in the Rabski Stream catchment – except for two sites in the Jabłonka River (Kita-Badak 1970, Rybak 2000).

The formation of arsenic mineralization in the Bystre Thrust-Sheet is associated with low-temperature hydrothermal fluids. Based on fluid inclusion studies, a minimum estimation of the crystallization temperature of realgar was determined at about 66°C (Jarmołowicz-Szulc et al. 2024). The source of fluids responsible for the mineralization occurring in the Bystre Thrust-Sheet could be (1) Neogene volcanic processes in eastern Slovakia (Wieser 1994) or (2) a hypothetical subvolcanic body (Nieć et al. 2016, Jarmołowicz-Szulc et al. 2023). This subvolcanic body is evidenced by a magnetic anomaly in the slice beds of the Dukla Nappe in the Slovak segment of the Outer Carpathians (Kucharič et al. 2012). The anomaly occurs approximately 35–40 km southeast of the Bystre Thrust-Sheet.

In the first cause, during the evolution of magma from alkaline to more acidic, as Wieser (1994) suggested, the solutions might be saturated with elements such as Hg, As, Sb or Cu

(Nieć et al. 2016). Along the south-western boundary of the Bystre Thrust-Sheet, a zone of strong tectonic deformations has been described ("tectonic mélange"; Jankowski & Jarmołowicz-Szulc 2009, Jankowski 2015). In this region, the zone could have contributed to intensive fluid migration (Jarmołowicz-Szulc & Jankowski 2021).

Such a large variety of metallic mineralization in rocks and tectonic structures, and particular mineralization with arsenic compounds, has an impact on the environment. Geochemical studies conducted on various environmental components in the Bystre Thrust-Sheet area have shown extensive arsenic geochemical anomalies in sediments and soils (Bojakowska & Borucki 1992, Rybak 2000). Studies of river sediments and catchment rocks have shown that arsenic predominates in sandstone and aquatic sediments' sand fraction (Rybak 2000, Wojciechowski 2003). The mineral waters found in the Bystre Thrust-Sheet are Poland's most eastern, CO_2-rich mineral waters. They were discovered thanks to boreholes drilled in the area of the "Anna" Spring – the Rabe-1 and the Rabe-3 boreholes. Their composition shows high concentrations of carbon dioxide, arsenic, and lithium compounds (Rajchel 2012).

RESEARCH AREA

The study covered surface and groundwater in southeastern Poland, at the mineralization region associated with arsenic compounds of the Bystre Thrust-Sheet. The study area is approximately 19 km^2 and belongs to the Western Bieszczady mesoregion (according to Solon et al. 2018) in the Outer Carpathians. This area is characterized by significant differences in relative heights with a typical vertical difference of 250–300 m over a distance of about 1 km. The slope gradient is usually 30° to 40°, although there are places where it reaches 60°, corresponding to relative slope gradients of 65–90%. Morphology, dense forestation and unsuitable conditions for the development of settlement, which could only occur in the valleys of the main streams (Organ 2021) resulted in the uninhabited the Bystre Thrust-Sheet area. There is no industrial or agricultural activity in this region. There are only two operating quarries: "Huczwice", also called "Drobny" (mining of Lgota sandstones) and the "Rabe" quarry, called "Gruby" (mining of thick-bedded Istebna sandstones). They both are located in the Rabski Stream valley (also known as Rabiański Stream; Fig. 1). Apart from quarries, occasional tree felling, and the transport network mainly along the Jabłonka River valley and the related road deicing system, there are no other potential direct sources of anthropogenic impact on the environment in the study area.

The study area is located in the Jabłonka River catchment area. The relative heights of the watersheds are asymmetrical – from the SW side, they are about 200 m, while from the E side 350–400 m, thanks to which the streams flowing through the Bystre Thrust-Sheet have a high erosion potential. Rabski Stream is a left tributary of the Jabłonka. In its valley, arsenic mineralization occurs directly on the surface (see Fig. 1). The stream has many smaller tributaries, and its beds are strongly incised, creating steep slopes. Mchawka is also a left tributary of the Jabłonka. The stream shows a small lithological variability of the substrate in the study area with the domination of calcareous layers (see Fig. 1). The only considered second-degree tributary of the Jabłonka is Huczwiczka, which feeds the Rabski Stream. The surface waters of the Bystre Thrust-Sheet are connected to the aquifers by a dense network of faults and fractures, which constitute migration paths for deeper, more mineralized waters. There are several springs in the Bystre Thrust-Sheet, where groundwater flows to the surface.

Most of the samples were collected from the four watercourses (Jabłonka, Rabski Stream, Mchawka and Huczwiczka) and their small tributaries. The rest of the samples were taken from natural springs, seeps and intakes made at the drilling sites (Fig. 1, Tab. 1). A dozen samples were also taken from streams located outside the Bystre Thrust-Sheet (Kołonica, Stężniczka, and some points at the Huczwiczka) to compare the results. Locations of points were collected during fieldwork in the ArcGIS Field Maps app and then fixed to 3-meter accuracy with a Garmin eTrex 10 GPS device. The detailed locations of the sampling points are shown in the table (Tab. 1; geographic position) and in Figure 2.

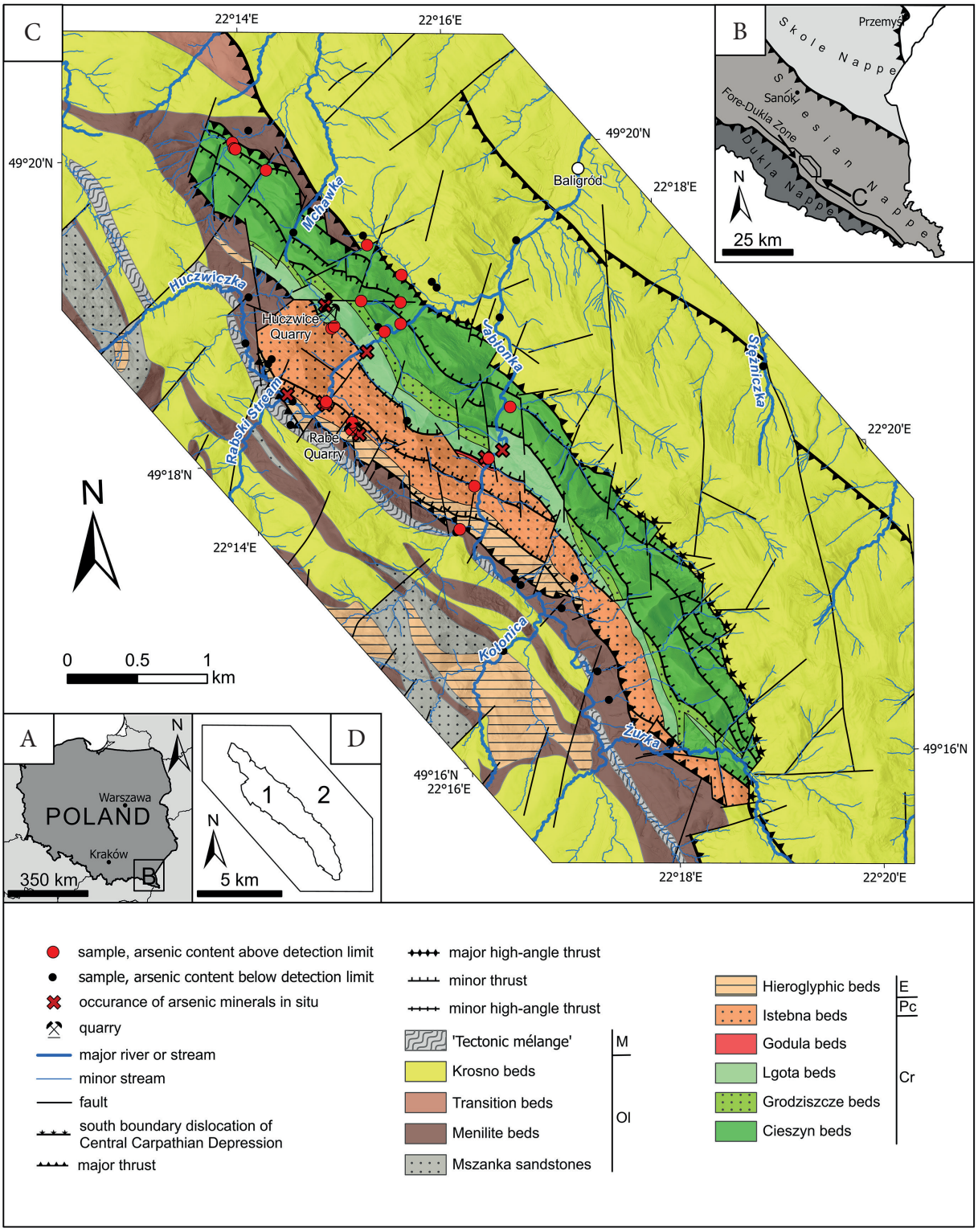

Fig. 1. *Location of study area: A) location of the research area on the map of Poland; B) location of the Bystre Thrust-Sheet on the map of eastern part of Western Outer Carpathians (modified after Świdziński 1958); C) geological map of the Bystre Thrust-Sheet and its vicinity with locations of sampled streams and springs (simplified stratigraphic chart with age limits: Cr – Cretaceous, Pc – Paleocene, E – Eocene, Ol – Oligocene, M – Miocene); D) division of map fields with the respect of source material (maps modified after: 1. Mastella 1995, Rybak 2000, 2. Malata et al. 1997, Jankowski & Ślączka 2000 – Krosno beds generalized; Layout modified after Jarmołowicz-Szulc et al. 2024)*

Table 1
Location and general characteristics of research points

Catchment	Point's symbol	Point's location	Type/ nature of water	Geographical position	
				N	E
Jabłonka River	J1	tributary stream	flowing	49.2733538	22.2894847
	J2	tributary stream	flowing	49.2784680	22.2878214
	J3	tributary stream	flowing	49.2865230	22.2847058
	J4	tributary stream	flowing	49.2833835	22.2824054
	J5	tributary stream	flowing	49.2860576	22.2758659
	J6	main stream	flowing	49.2867043	22.2750302
	J7	tributary stream	flowing	49.2919739	22.2656912
	J8	tributary stream	flowing	49.2922890	22.2663074
	J9	tributary stream	flowing	49.2968324	22.2690181
	J10	Bystre 1 borehole	intake	49.2997290	22.2715129
	J11	tributary stream	flowing	49.3051441	22.2754225
	J12	main stream	flowing	49.3103901	22.2760601
	J13	ORW Bystre	intake	49.3147657	22.2743478
	J14	'near chapel'	spring	49.3229462	22.2775960
Rabski Stream	R1	near Synarewo chapel	spring	49.3042120	22.2393335
	R2*	Rabe Quarry little lake	standing	49.3034357	22.2492627
	R3*	Rabe Quarry heap leakage	flowing	49.3042032	22.2494828
	R4**	"Anna" Spring	spring	49.3063600	22.2453035
	R5	Rabe-1 borehole	spring	49.3060030	22.2448440
	R6	tributary stream	spring	49.3041268	22.2584392
	R7	Huczwice Quarry	intake	49.3143681	22.2467400
	R8*	Huczwice Quarry – water drainage	flowing	49.3145849	22.2471832
	R9***	Huczwice Quarry – natural outflow	spring	49.3177997	22.2464974
	R10	tributary stream	flowing	49.3142965	22.2543881
	R11	main stream	flowing	49.3137589	22.2553791
	R12	tributary stream	spring	49.3171683	22.2517681
	R13	tributary stream	flowing	49.3145358	22.2580648
	R14	'calcareous sinter' – little flow	spring	49.3168272	22.2581901
	R15	tributary stream	flowing	49.3241442	22.2525295
	R16	tributary stream	flowing	49.3231192	22.2531341
	R17	anthropogenic tributary from intake	flowing	49.3197397	22.2585616
	R18	tributary stream	flowing	49.3188929	22.2634836
	R19	tributary stream	flowing	49.3182498	22.2642453
Huczwiczka Stream	H1	tributary stream	flowing	49.3180643	22.2333676
	H2	main stream	flowing	49.3131590	22.2325296
	H3	tributary's spring	spring	49.3113405	22.2367040
	H4	tributary stream	flowing	49.3108637	22.2361034
	H5	main stream	flowing	49.3067337	22.2398456
Mchawka Stream	M1	tributary stream	flowing	49.3315893	22.2371145
	M2**	"Karolina" Spring	spring	49.3339789	22.2322401
	M3**	near Roztoki Dolne	spring	49.3340666	22.2319878
	M4	tributary stream	flowing	49.3346810	22.2317798
	M5	private estate	intake	49.3359094	22.2345029
	M6	main stream	flowing	49.3247087	22.2412960
Kołonica Stream	K1	main stream	flowing	49.2790899	22.2725815
Stężniczka Stream	S1	main stream	flowing	49.3083116	22.3171117
Żurka Stream	Z1	"Żurka" Spring	spring	49.2685519	22.2992579

* drainage of exploited rocks from quarries, anthropogenic impact;

** occurrence of the characteristic white sediment related to the sulphur-reducing bacteria;

*** spring outflowing directly from Lgota beds on the higher levels of the Huczwice Quarry (other springs begin their flow on the surface in quaternary deposits).

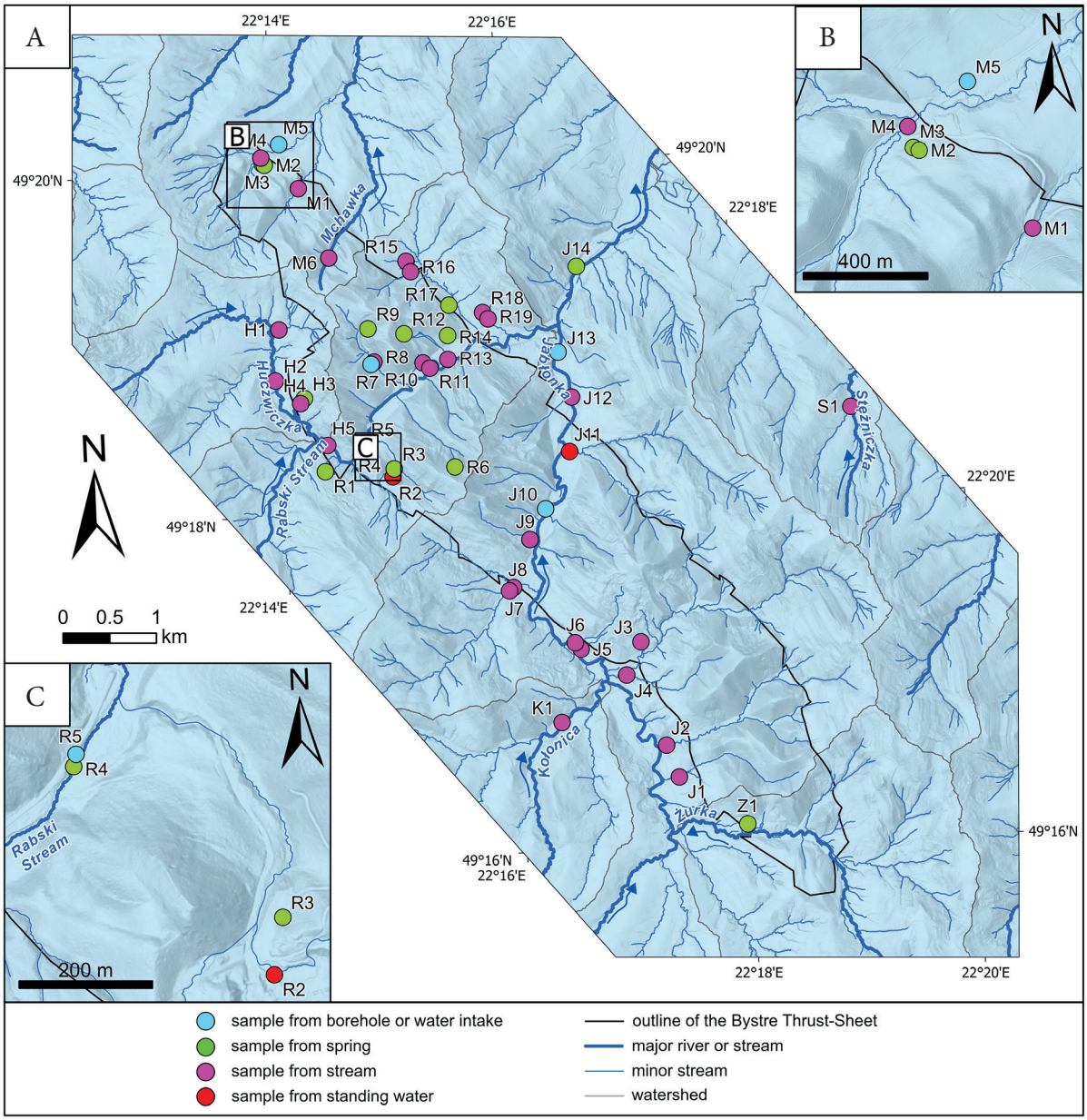

Fig. 2. *Location of sampling points (markings following Table 1): A) all sampling places in the individual catchments; B) detailed locations for some points in the Mchawka Stream catchment; C) detailed locations for some points in the Rabski Stream catchment*

MATERIALS AND METHODS

Water samples were collected over four days in June 2023 at 47 research points from the shore directly into clean polypropylene bottles. For selected sites, repeat arsenic determinations were performed in the following year (in August 2024) to check for seasonal variability. At each point, three subsamples were obtained. The first one was unfiltered, the second was filtered, and the third was acidified after filtration. For filtration, single-use cellulose acetate syringe filters of 0.45 μm were used. Ultrapure nitric acid 65% was used to acidify water to a pH below 2. Each sample was kept in a refrigerator at 4°C until analysed (according to the European Standard PN-EN ISO 5667-3:2024). The pH (pH meter, Elmetron CP-105; GP-105; accuracy ±0.02), redox potential (Eh, Elmetron CP-105; GR-105k; accuracy ±1.0 mV), temperature (Elmetron CP-105; accuracy ±0.08°C),

electrical conductivity (EC, Elmetron CC-105; accuracy ±1%) were measured *in situ*.

Major cations and elements were analysed using an inductively coupled plasma mass spectrometer (ICP-MS, ELAN 6100, PerkinElmer) or an inductively coupled plasma optical emission spectrometer (ICP-OES, Plasm 40, Perkin Elmer) in a certified Hydrogeochemical Laboratory (PCA certificate, no AB 1050) in the AGH University of Science and Technology in Krakow. Chlorides and bicarbonates were determined using titrimetric methods according to the following standards: chlorides – PN-ISO 9297:1994 (Mohr's method) and bicarbonates – PN-EN ISO 9963-1:2001+Ap1:2004.

The maps (Figs. 1, 2 and 8) were created using ESRI ArcGIS Pro software. LiDAR data, obtained from the Head Office of Geodesy and Cartography (GUGiK) database, was used as the topographic base. Watersheds within the location map (Fig. 2) were delineated using the Watershed tool (Spatial Analyst) in ArcGIS Pro. To construct Figures 1, 2 and 8, a compilation of several maps of the study area was made based on publication by Mastella (1995), vide Rybak (2000), Malata et al. (1997), Jankowski & Ślączka (2000) and Jarmołowicz-Szulc et al. (2023).

The Piper diagram was made using The Geochemist's Workbench software. The hydrogeochemical type of water was determined (Alekin 1970) based on (Rajchel 2012) in accordance with the Szczukariew–Priklonski classification. StatSoft Statistica software was used for statistical analyses of correlations and calculations of statistics for individual analysed parameters. The Shapiro-Wilk test (Shapiro & Wilk 1965) for individual physicochemical parameters and analysed substances is statistically significant ($p < 0.05$), which means that the distribution of these data deviates from the Gaussian distribution (except for Ca^{2+}, with $p > 0.05$). This feature is also confirmed by graphical observation of the histograms of individual parameters. This means that the analysed data statistically do not show a normal distribution, therefore they are not parametric. Hence, the calculation of the correlation coefficient matrix was performed for the Spearman correlation (Spearman 1904).

Data quality control

Optimum purity conditions were used for all analyses to avoid sample contamination. All of the equipment used was thoroughly rinsed with deionized water before use. Analyses were performed according to standard certified analytical quality control procedures (PN-EN ISO 17294-1:2007 and PN-EN ISO 11885:2009). Reagent blanks and certified reference materials were used to control analytical accuracy. Repetitions were performed, the mean value and analysis errors were calculated.

RESULTS

Due to the presence of arsenic compounds in rocks, aquatic sediments, and mineral waters, it was checked to what extent arsenic penetrates into waters and how far from its potential sources does a clear geochemical anomaly appear. The main objective of the study was to check the presence and range of arsenic in water but other physical and chemical properties of water were also determined. They aimed to recognize mutual dependencies that will allow for a better understanding of the genesis of this metalloid in water and to identify the conditions that affect the behaviour of arsenic in the aquatic environment. The study area consists mainly of small watercourses, primarily streams collecting water from the catchment area belonging to the Bystre Thrust-Sheet (Figs. 1 and 2). The statistical description of the most important physicochemical properties of water is listed in Table 2. In total, the values/contents of 36 indicators were determined. However, many of them were below the detection limit of the method used; therefore, they were not taken into account in the table. The results were compared to the values indicated as thresholds for the first class of surface water quality (by the law in force in Poland, which is consistent with EU guidelines).

Differences of arsenic concentration depending on the physicochemical properties of water

Arsenic concentration (above the detection limit) in twenty water samples varied within wide range (1.05–378.72 μg/L; Tab. 2). In eight samples, it exceeded the value of 10 μg/L, which is the threshold recommended by the World Health Organization for drinking water (WHO 2022), while in four samples exceeded the value of 50 μg/L, which corresponds to the permissible value specified

in the ministerial regulation first quality class of surface water in Poland (*Rozporządzenie…* 2021). Its concentrations above the detection limit occurred only in some, described below (see also Tab. 2), quite specific places at twenty sampling points and in the basin areas of three river courses (Jabłonka River, Rabski Stream and Mchawka Stream). All these sites were localized in the Bystre Thrust-Sheet area.

In the **Jabłonka River** basin area, these were either its small tributaries (J8, J9, and J11) or the water outflow from the Bystre 1 borehole (J10, Figs. 2 and 3). In the case of point J10, the obtained concentration (378.72 μg/L) was the highest for the entire studied area (Tab. 2) and significantly exceeded the permissible value (50 μg/L). It should be noted that the water at the borehole's outlet has high electrolytic conductivity value (EC, 715 μS/cm), high content of total dissolved solids (TDS, 1,023.57 mg/L), bicarbonates (455.28 mg/L), chlorides (14.73 mg/L), sodium (122.28 mg/L), potassium (9.88 mg/L), fluorides (3.09 mg/L), lithium (264.30 μg/L) contents, and pH value (7.85) indicating the alkaline nature of the water.

In the case of the catchment area of the second watercourse – **Rabski Stream**, there are four specific places where arsenic appears in the water. The first of them are located close to points R2-R5 (Fig. 2).

Table 2
Statistical description of the physicochemical parameters of the analysed waters

Parameter	*n**	Min.	Max.	Arithmetic mean	Standard deviation	25th percentile	Median	75th percentile	Guideline value**
pH [–]	37	3.33	8.40	–	–	6.58	7.27	7.70	7.80–8.40
Eh [mV]	9	–297.20	437.00	–	–	111.60	153.50	357.80	n.e.***
EC [μS/cm]	39	81.00	2,670.00	526.53	557.14	260.00	398.00	470.00	192.00
TDS [mg/L]	47	12.24	4,549.96	438.87	700.30	186.48	296.12	380.32	118.00
Macroions [mg/L]									
Calcium	47	4.21	109.40	47.81	27.39	21.37	50.68	70.18	50.00
Magnesium	47	0.91	35.18	9.79	7.81	4.84	7.57	12.03	5.30
Sodium	47	0.51	1,220.00	63.49	206.76	0.96	1.87	5.79	n.e.
Potassium	47	0.49	33.27	2.74	5.24	0.98	1.25	1.77	n.e.
Fluorides	37	0.04	3.09	0.66	0.66	0.09	0.52	0.90	1.50
Chlorides	47	2.12	692.70	31.96	111.07	2.69	2.83	5.24	3.00
Bicarbonates	44	21.80	2,502.00	301.67	408.17	149.08	221.33	268.35	n.e.
Sulphates	47	1.50	255.34	28.08	44.29	11.36	16.84	25.37	17.20
Silicates	4	7.93	13.28	9.93	2.50	8.02	9.25	11.84	n.e.
Trace metals/metalloids [μg/L]									
Aluminium	7	11.66	2,670.00	794.72	1,127.94	34.87	231.19	2,185.68	400.00
Arsenic	**20**	**1.05**	**378.72**	**38.94**	**88.28**	**1.53**	**3.95**	**20.23**	**50.00**
Barium	44	21.43	11,270.00	475.14	1,733.06	58.99	75.43	105.54	500.00
Copper	6	1.14	13.00	4.42	4.74	1.32	2.03	7.02	50.00
Iron	30	10.28	1,230.00	115.09	248.83	13.39	16.39	112.32	n.e.
Mercury	4	0.13	0.57	0.30	0.20	0.15	0.25	0.45	0.07
Lithium	30	5.65	1,860.00	127.70	364.05	7.29	9.25	14.84	n.e.
Manganese	3	178.00	2,871.96	1,616.85	1,356.31	178.00	1,800.00	2,871.96	n.e.
Lead	5	0.29	1.08	0.63	0.37	0.33	0.58	0.94	14.00
Strontium	14	86.00	2,370.00	564.04	567.58	246.23	426.37	662.57	n.e.
Zinc	3	14.50	325.83	118.44	179.60	14.50	15.00	325.83	100.00

* number of results above detection limit;

** 1st class according to *Regulation on the classification of ecological status, ecological potential, chemical status and the method of classifying the status of surface water bodies as well as environmental quality standards for priority substances* (*Rozporządzenie…* 2021; for a stream or small flysch river – of a silicate or carbonate nature);

*** not established;

Explanations: EC – electrical conductivity, TDS – total dissolved solids

Points R2 and R3 are places associated with quarries, where water accumulates in depressions, both washed out from rocks and directly from atmospheric precipitation. However, in these places, the As content does not exceed 2.5 µg/L. This water has an exceptionally low pH (4.10) and a relatively higher sulphate content (60.28 mg/L) which may be the reason for arsenic precipitation and binding in the sediment (Moore et al. 1988, Cullen & Reimer 1989). At points R4 and R5 we are dealing with outflows from below the ground surface. Near point R4 (as well as in M2 and M3 points – Fig. 4), a specific white precipitate appears on the ground surface. It is assumed that it is related to the activity of sulphur bacteria (cf. Rajchel et al. 2002). In these places, the As content exceeds 20 ug/L. At point R5 (borehole) very high (the highest in the studied area; Tab. 2) contents of barium (11.27 mg/L), chlorides (692.70 mg/L), bicarbonates (2,502.00 mg/L), potassium (33.27 mg/L), lithium (1.86 mg/L), and sodium (1,220.00 mg/L) occurred which is reflected in a very high TDS content (4,568.06 mg/L). In the next location R7 and R8, the concentration of arsenic is indeed determined, but it is not high and does not exceed 18 µg/L. This is again the area of the quarry – Huczwice. In this place, the waters have a high content of calcium (109.40 mg/L), magnesium (35.18 mg/L) and sulphates (85.23 mg/L) that significantly exceed the permissible values and a high pH value (8.40). The third place is located close to points R11-R14, where only point R14 has a high As content (137.00 µg/L), and in the remaining points it does not exceed 5.00 µg/L. At point R14, a calcareous sinter was observed on the surface. The water contains high calcium ion content (97.86 mg/L), which may be responsible for this phenomenon, and at the same time for the pH (7.70) which gives the water an alkaline character. In the fourth place (R16 and R17) arsenic occurs in contents above the detection limit, but these are very low concentrations (about 1 µg/L). At the same time, the waters in these places have a high pH (8.05) and relatively high calcium ion contents (approximately 78 mg/L).

Fig. 3. *The Bystre 1 borehole secured with green pipe (point J10, for location see Tab. 1 and Fig. 2); a backpack as the scale*

Fig. 4. *White precipitate on the ground surface in the area of spring near the Roztoki Dolne village (point M3, for location see Tab. 1 and Fig. 2); pH-meter as the scale*

Arsenic was also detected in the **Mchawka Stream** catchment, at points M1-M4, whereby at points M1 and M4 (flowing waters) the concentrations of this element are not high (below 3.5 µg/L). At points M2 and M3 there were small natural water springs. In these places, a white precipitate could also be seen on the ground surface (Fig. 5). Arsenic contents in these places reach up to 106 µg/L. The waters also have high contents of chlorides (up to 138.80 mg/L), bicarbonates (up to 1,040.70 mg/L), lithium (up to 0.44 mg/L), sodium (up to 499.88 mg/L), EC (up to 2,300 µS/cm) and TDS (up to 1,817.49 mg/L).

Analyzing the results of repeated analyses for selected locations, it was found that the differences between changes in the content of individual elements vary depending on the area and the component (Tab. 3). Generally, the highest seasonal variability for sites having direct contact with rainwater and access to atmospheric air (R2 and R3 – quarry location, and J9 – stream) was observed. In the case of water from springs and boreholes (R4, R5, J10, and M2) this variability is smaller. The content of lithium and sodium remained at a similar level in all analyzed places.

Fig. 5. *The Rabe quarry (called "Gruby") with the water accumulated in depressions (point R2, for location see Tab. 1 and Fig. 2)*

Table 3
Changes of some elements in the selected places (for location see Figs. 1 and 2, as well as Tab. 1)

Element	Year	R2	R3	R4	R5	J9	J10	M2
As^{3+} [µg/L]	**2023**	10.50	2.40	12.20	21.00	19.46	378.70	60.15
	2024	15.30	43.23	13.28	9.55	21.54	356.71	54.99
Ba^{2+} [µg/L]	2023	40.00	30.00	2,810.00	11,270.00	30.00	1,020.00	1,310.00
	2024	90.00	90.00	4,720.00	11,410.00	90.00	1,080.00	1,570.00
Ca^{2+} [mg/L]	2023	21.37	15.34	10.98	50.68	4.21	24.70	15.40
	2024	16.59	27.60	28.30	47.73	8.60	35.23	32.96
Li^{+} [mg/L]	2023	0.02	0.01	0.61	1.86	0.01	0.26	0.30
	2024	0.01	0.02	0.67	1.75	0.01	0.26	0.31
Na^{+} [mg/L]	2023	1.87	1.47	407.41	1,220.00	1.31	122.28	346.33
	2024	1.87	2.35	438.64	11,66.09	2.27	118.42	344.71
SO_4^{2-} [mg/L]	2023	180.60	108.15	4.41	3.24	9.06	<1.00	<1.00
	2024	176.90	209.11	30.57	10.21	14.91	<1.00	<1.00

Correlations between analysed water parameters

Spearman's correlation coefficient value was calculated to check the relationship between various parameters (Tab. 4). If the correlation coefficient between two elements is high (close to 1), this may indicate their common origin or similar distribution. A high correlation was found between Eh and other parameters such as EC, TDS, HCO_3^-, Na^+, Ba^{2+}, Cl^-, Li^+ (negative correlation) and SO_4^{2-} (positive correlation), showing that in oxygenated waters the value/content of other parameters decreases. The exception is sulphates, the concentration of which increases, which is most likely due to the oxidation of sulphides. A high or very high positive correlation was found between HCO_3^- and EC, TDS and Sr^{2+}. Strontium also correlates strongly with other indicators such as EC, TDS, As^{3+}, Ba^{2+}, HCO_3^-, Li^+, Na^+, and SO_4^{2-}.

Attention should be paid to arsenic, which correlates moderately positively with lithium, strontium, fluorides, and chlorides but negatively with sulphates. There are also some specific groups of indicators showing slightly weaker but clear interrelationships. The first group including SO_4^{2-}, Ca^{2+} and Mg^{2+} can be connected with weathering of sulphides. The second group HCO_3^-, Ca^{2+}, and Mg^{2+} may result from the washing out of weathered surface carbonate rocks by infiltrating rainwater. The presence of the last group HCO_3^-, Cl^- and Na^+ is most likely due to the dissolution of the mineral components of the substrate by groundwater.

Table 4

Spearman correlation coefficients between pars of elements for analysed water samples

Parameter	pH	Eh	EC	TDS	As^{3+}	Ba^{2+}	Ca^{2+}	Cl^-	F^-	HCO_3^-	K^+	Li^+	Mg^{2+}	Na^+	SO_4^{2-}	Sr^{2+}
pH	x	9	34	37	17	36	37	36	29	36	37	24	37	37	37	10
Eh	−0.15	x	**9**	**9**	9	**8**	9	9	6	**9**	9	8	9	**9**	**9**	5
EC	0.16	**−0.87**	x	**39**	**19**	**38**	**39**	**37**	**36**	**37**	39	**25**	**39**	**39**	39	**12**
TDS	0.24	**−0.88**	**0.92**	x	**20**	**46**	**47**	**44**	**37**	**44**	47	**30**	47	**47**	47	**15**
As^{3+}	0.05	−0.30	**0.48**	**0.48**	x	**19**	20	**19**	**14**	**19**	20	**15**	20	20	**20**	**10**
Ba^{2+}	0.17	**−0.83**	**0.67**	**0.63**	**0.46**	x	46	**43**	37	**43**	46	**30**	46	**46**	46	15
Ca^{2+}	0.24	−0.07	**0.37**	**0.43**	−0.36	0.25	x	44	37	**44**	**47**	30	**47**	47	**47**	15
Cl^-	0.09	**−0.65**	**0.52**	**0.54**	**0.47**	**0.37**	0.00	x	34	**44**	44	**28**	44	**44**	44	**15**
F^-	−0.14	−0.31	**0.41**	**0.42**	**0.62**	0.23	−0.13	0.30	x	**34**	**37**	**23**	37	**37**	37	10
HCO_3^-	0.14	**−0.87**	**0.90**	**0.95**	**0.54**	**0.79**	**0.39**	**0.46**	**0.46**	x	44	**28**	**44**	**44**	44	**15**
K^+	−0.10	−0.53	0.09	0.13	**0.39**	0.19	**−0.41**	0.27	**0.55**	0.09	x	**30**	47	47	47	**15**
Li^+	**−0.39**	**−0.69**	**0.55**	**0.52**	**0.53**	**0.57**	−0.25	**0.53**	**0.67**	**0.68**	**0.52**	x	30	**30**	30	**13**
Mg^{2+}	−0.01	0.32	**0.37**	**0.56**	−0.20	0.04	**0.35**	0.16	0.26	**0.37**	−0.02	0.16	x	**47**	**47**	15
Na^+	0.03	**−0.78**	**0.56**	**0.69**	0.32	**0.47**	0.02	**0.45**	**0.54**	**0.66**	0.19	**0.61**	**0.63**	x	47	**15**
SO_4^{2-}	−0.07	**0.69**	0.08	0.14	**−0.57**	−0.17	**0.60**	−0.09	0.07	−0.02	−0.24	−0.26	**0.59**	0.02	x	**15**
Sr^{2+}	0.13	−0.20	**0.82**	**0.75**	**0.71**	**0.92**	−0.33	**0.61**	0.50	**0.80**	**0.59**	**0.84**	−0.36	**0.78**	**−0.78**	x

Explanations: the left part (green): Spearman correlation coefficients; the right part (blue): the number of pairs included in correlation calculations. Bolded values represent statistically significant correlation ($p < 0.05$) and marked in red colour point to very strong correlation coefficients. EC – electrical conductivity, TDS – total dissolved solids

DISCUSSION

The chemical composition of surface water is dependent on many natural and anthropogenic factors in the drainage basin and hence is characterized by high variability and is particularly pronounced in the case of watercourses, for which the dynamics of changes are largely dominated by the

variability of other elements of the aquatic environment (e.g. Aleksander-Kwaterczak & Plenzler 2019). This composition and its changes depend primarily on the geological structure of the catchment area, hydrometeorological conditions, and seasonal dynamics of river runoff (Shomar et al. 2005, Sajdak et al. 2018, Borek 2024) and are generally most visible when the levels of water are low (Bartram & Balance 1996).

Division of waters depending on ionic composition

On the basis of correlation results and by creating a Piper diagram illustrating the relationships between the main ions (Fig. 6), the analysed waters were classified into three basic types. Based on the literature's data (Rajchel 2012), the origin of individual water types can also be determined. Waters characterized by the ionic type SO_4-Ca or SO_4-Ca-Mg are associated with the weathering of sulphides in the near-surface hypergenic zone. Rocks exposed on the surface and their additional fragmentation due to mining operations conducted in quarries impact it. This is an infiltration kind of water that flows through weathering rocks. During the infiltration process metal ions and sulphates, occurring after sulphur oxidation, can then get into it.

This group (Fig. 6; group A) consists of six water samples collected within the Rabski Stream's catchment area (R2, 3, 6, 8, 10, and 11). These waters have some of the lowest TDS, averaging 153.85 mg/L ±157.25 mg/L and are also characterized by low pH, with a median of 5.61 (min. 3.33). However, one sample from outside of the quarry area has the highest pH value among all research samples (8.40). The arsenic concentration in these samples is the lowest among all groups (1.77 mg/L ±0.70 µg/L, median: 1.82 µg/L).

In waters with the HCO_3-Ca or HCO_3-Ca-Mg ionic type the main supplying component is rainwater, infiltrating shallowly into the rock mass, where within the well-permeable rocks (porosity, especially fractures) they move quickly. This causes a short contact of water with the rocks, which is why they are very poorly mineralized. Rajchel (2012) considered mainly carbonated waters within this group. However, it seems justified to include flowing surface waters that interact the ground only within Quaternary formations in this group.

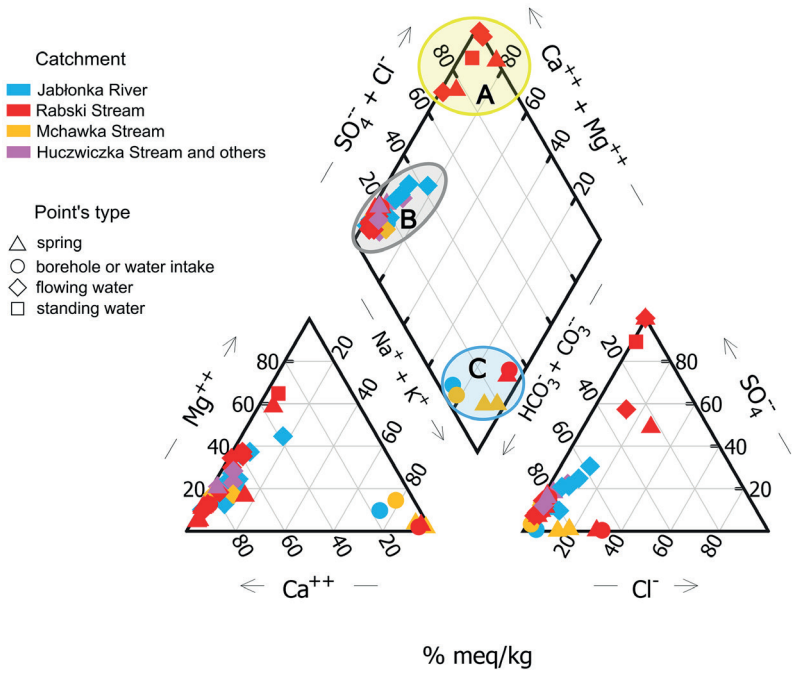

Fig. 6. *Relationships between the main ions in the analysed watercourses on the Piper diagram. Types of water: A – SO_4-Ca-Mg; B – HCO_3-Ca-Mg and C – HCO_3-Cl-K/Na (with a substantial addition of Cl^- ions due to anions triangle – even to about 40% meq/kg of anion content)*

This group (Fig. 6; group B) includes the most typical infiltrative waters, which do not provide directly significant insight into the mobility and origin of arsenic in the waters. These waters exhibit low average mineralization of 265.03 mg/L ±109.81 mg/L, with average arsenic content of 17.60 µg/L ±40.13 µg/L (median: 3.22 µg/L). They are also characterized by rather neutral pH, with a median of 7.29 (min. 5.20). In this group water samples from the catchment of three watercourses: Jabłonka (J8, 9 and 11), Rabski Stream (R7, 12–14, 17–18) and Mchawka (M1 and 4) were included.

Waters of the HCO_3-Na or HCO_3-Cl-Na ionic type originate from the displacement of higher mineralized diagenetic, synsedimentary or paleoinfiltration waters by infiltration waters. Ca-Na ion exchange occurs, and lighter groundwater (due to the high content of gaseous CO_2) are pushed towards the surface, sometimes in the form of surface outflows (Rajchel 2012).

This group (Fig. 6; group C) includes six samples located in each of the major catchments within the study area (J10, R4, R5, M2, M3, and M5). These waters are highly mineralized, with TDS ranging from 647.52 mg/L to 4,549.96 mg/L and characterized by the most alkaline pH, from 6.49 to 7.85 with a median of 7.41. They also show the highest arsenic concentrations among all chemical water types in the Bystre Thrust-Sheet, ranging from 12.21 µg/L to 378.72 µg/L (115.60 µg/L ±151.69 µg/L). In each case, these are either groundwater samples, extracted to the surface through boreholes Rabe-1 and Bystre 1 (R5 and J10), groundwater from local, domestic water intakes (M5), or groundwater emerging at the surface as mineralized springs (R4, M2 and M3).

Origin of arsenic in waters

Analysing the results obtained in this work, it was found that the most probable genesis of arsenic in waters is the dissolution of arsenic minerals occurring in intensively mineralized zones of realgar, the presence of which was found during mapping of the area (Fig. 7). Synsedimentary waters displaced by infiltrating rainwater are rich in TDS and free carbon dioxide, therefore they behave as aggressive solutions and can dissolve arsenic minerals more easily than typical surface waters. There are known acidic waters which, thanks to their high content of free carbon dioxide, can dissolve even silica (Rajchel 2012). Arsenic minerals have a lower solubility constant than quartz (Lu & Zhu 2011), which is why the dissolution of these minerals is possible through the migration of groundwater occurring in the study area. This is additionally supported by the high arsenic content in waters belonging to the HCO_3-Na or HCO_3-Cl-Na ionic type (Fig. 6; group C of the Piper diagram) and the values of correlation coefficients (0.46–0.71) of arsenic with Ba, Cl, F, HCO_3^-, Li and Sr.

Arsenic probably enters surface waters to a lesser extent through the arsenic minerals' weathering in the hypergene zone. It is reflected in the lack of correlation between arsenic and the most important components of meteoric waters, i.e. Ca and Mg. In the case of A and B ionic type groups (Fig. 6) arsenic contents in surface water are much lower than in groundwater, perhaps partly due to short contact of water with arsenic mineral zones. In quarries, arsenic minerals' weathering should result in higher arsenic contents in water but that is not the case. Its lower contents may be related to arsenic precipitation into the sediment at high sulphate contents, originating from sulphide weathering.

The presence of arsenic-containing water confined to the Bystre Thrust-Sheet area highlights a strong connexion between arsenic concentrations in water, arsenic mineralization, and tectonic processes (Fig. 8). The deep circulation of carbonate and CO_2-rich waters likely follow the same migration pathways as the fluids responsible for arsenic mineralization.

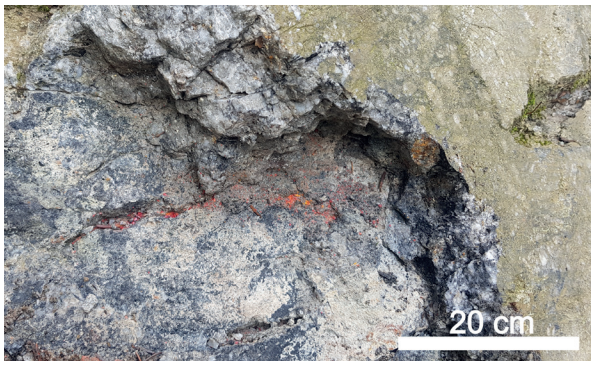

Fig. 7. *Realgar (red colour) in the fault zone in the Rabe valley within the Bystre Thrust-Sheet area*

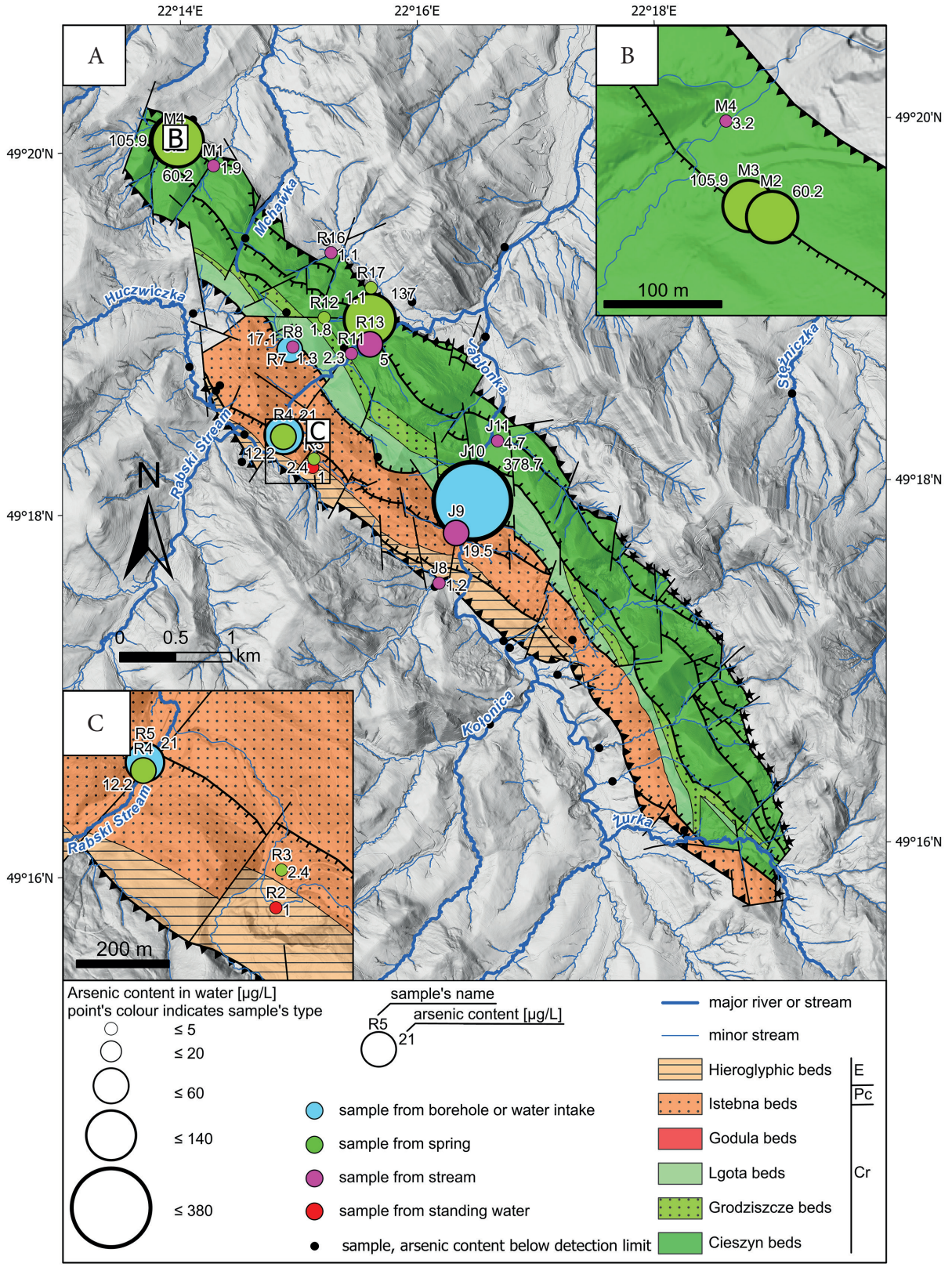

Fig. 8. *Arsenic content in water presented spatially concerning the different types of samples (the Bystre Thrust-Sheet map modified after Mastella 1995, Rybak 2000; simplified stratigraphic chart with age limits: Cr – Cretaceous, Pc – Paleocene, E – Eocene): A) results for all sampling places in the individual catchments (markings following Table 1); B) results for some points in the Mchawka Stream catchment; C) results for some points in the Rabski Stream catchment*

The influence of physicochemical and geological conditions on the behaviour of arsenic in the aquatic environment

The pH is one of the most important parameters which may change the bioavailability and toxicity of metals (Boyd 2015, Ciszewski & Aleksander-Kwaterczak 2020). Low pH values can weaken metal bonding strength and hinder metal retention in the solid phase, while high pH values can cause metal adsorption and precipitation, making them undetectable in overlying waters (Guven & Akinci 2013, Zhang et al. 2014). The pH of analysed waters falls within a very wide range from 3.33 to 8.40 (Tab. 2). Acidic waters (pH < 6.5) appeared in places associated with spoil heaps in quarries, i.e. they were related to the weathering of all kinds of sulphides, mainly pyrite, as well as in the small Huczwiczka Stream. High pH values (from 8.0 to 8.5, less frequently 9.0) occurred in waters associated with the rocks containing a significant share of calcium carbonate, mainly in the Cieszyn beds. Lower concentrations of As in flowing waters in areas where the Cieszyn beds occur as well as lack of arsenic in these waters after passing the Cieszyn beds may be related to the strongly calcareous character of these beds. The limestone decreased soluble As due to increased pH (cf. Veloso et al. 2019). It means that these beds form a natural barrier to the migration of arsenic outside the Bystre Thrust-Sheet.

The second important parameter is the oxidation-reduction potential (Eh), the increase of which causes faster oxidation of sulphides and degradation of organic sediment compounds, which will cause the release of metals and metalloids bound in them (Peng et al. 2009). Changes in Eh, occurring for example as a result of large and/or long-term changes in water levels, may in turn affect pH values (Frohne et al. 2011). The Eh of water varied between –297.2 and +437.0 mV (Tab. 2). Negative Eh values were only marked in places where a white precipitate appeared on the surface due to the presence of sulphur-reducing bacteria. Positive values of Eh prevailed in the vast majority of places and such values evidenced oxidizing conditions and are characteristic for well-aerated water. This situation favours the processes of self-purification of water but also facilitates the oxidation and dissolution of solid components present at the bottom.

The diversity of EC values of surface waters is largely influenced by the geological structure and amount of precipitation (Boyd 2015). In our study, the results of conductivity measurements ranged between 81.00 and 2,670.00 μS/cm (Tab. 2). High values may result from leaching rock components and from anthropogenic activities to a much lesser extent. Considering the relationships between individual elements, a strong relationship between EC and TDS can be observed, which may indicate a large impact of water mineralization on specific electrolytic conductivity. To a lesser degree, it may also result from the presence of salt in the environment, which is used to de-ice roads and is consequently washed out of the catchment area into the water.

Taking into account the concentration of arsenic in the water flowing to the surface from below the ground and in the water of watercourses, one can see the local influence of geological conditions on the concentration of this metalloid. Relatively high concentrations of arsenic appeared only in springs and boreholes. In flowing waters, these concentrations quickly decreased either due to dilution or precipitation and binding to the solid phase. The conditions predominant in waters, mainly high pH, favour the immobilization of metals in sediments and suspended matter. This was confirmed by the studies of alluvial sediments conducted by Bojakowska & Borucki (1992). Due to the fact that they were conducted quite a long time ago, it would be advisable to repeat them.

The situation may only be dangerous in the case of acidification of the environment, for example due to oxidation of sulphides (cf. Veloso et al. 2019). Lowering the pH may cause the remobilization of metals/metalloids from the solid phase to the solution. Another threat may be caused by a drastic decrease in water levels due to prolonged drought since pollutants will not then be diluted. On the other hand, heavy and prolonged rainfall may cause the sediments to be carried away from the place of their deposition and cause the dispersion of pollutants in the valley of watercourses.

The presence of arsenic in spring water, even in areas lacking surface mineralization, suggests

deep-seated arsenic mineral deposits, indicating a more extensive mineralization zone than previously mapped. The observed As concentration in water from the Bystre Thrust-Sheet area is relatively low. Locally, exploiting mineralized zones in quarries contribute to increased arsenic concentration in surface waters. This impact probably depends on weather conditions and the extent of the exploitation. Much higher concentrations of arsenic (3,778 μg/L) in water in Poland were detected in the Trująca Woda Stream in Lower Silesia in the area affected by geogenic arsenic contamination (Komorowicz & Barałkiewicz 2016). It is closely related to the extraction of arsenic ores, which was accompanied by gold in the Złoty Stok As-Au deposit area (Sudetes).

The same contamination is observed in the area of abandoned antimony mines in the Western Carpathians (Slovakia). Mine wastes are a source of arsenic in water of different types. The observed concentrations of As are elevated up to 2,150 μg/L (Hiller et al. 2012). The cases described above show how the exploitation of deposits containing arsenic can result in aquatic environmental pollution. The change in arsenic content in sample R3 is likely related to the reactivation of mining at the Rabe (Gruby) quarry, which contributed to the intensification of the weathering process (including arsenic minerals). The exposure of mineralized zones thus significantly affects the composition of surface waters and shallow circulating groundwater. This means that the quarry area in the Bystre Thrust-Sheet should be particularly monitored for arsenic contamination.

The potential use of waters from the Bystre Thrust-Sheet area for health resort purposes

Many years of tests of water from the Rabe-1 borehole (near Baligród) have shown that it meets the criteria of 0.48% bicarbonate-chloride-sodium, boron acidic water (Łach & Pasztyła 2013). The authors drew attention to the presence of microelements such as arsenic, lithium and iron in these waters, which are very rarely found in such a combination. Arsenic waters used for health resort purposes contain this element primarily in arsenic acid compounds or arsenites. This metalloid stimulates the hematopoietic activity of the bone marrow and inhibits the overall metabolism (Litwin et al. 2009). On the other hand, human exposure to arsenic from various sources, including high contents of this potentially toxic element in groundwater, has become a serious global problem (Chung et al. 2014, Chaudhary et al. 2024). The main diseases that may result from arsenic poisoning include cancer, hypertension and diabetes (Hall 2002, Fatoki & Badmus 2022).

The analysed deep waters contain components that, at appropriate concentrations, may positively affect human health. A very interesting example is the Bystre 1 borehole ("Danuta" Spring; J10). The water at the borehole's outlet is alkaline (pH = 7.85) and has high content of total dissolved solids (TDS, 1,023.57 mg/L), bicarbonates (455.28 mg/L), chlorides (14.73 mg/L), sodium (122.28 mg/L), potassium (9.88 mg/L), fluorides (3.09 mg/L) and lithium (264.30 μg/L). These waters could therefore be used as a valuable source of micro- and macroelements. However, high arsenic concentrations (378.72 μg/L) may preclude their use. A similar situation occurs in the case of two springs in the Mchawka Stream valley, where high arsenic concentrations (about 60 μg/L and 106 μg/L) and similar water types were also found (Tab. 4).

However, water from two other places has great health resort potential: the "Anna" Spring (R4) and the Rabe 1 borehole (R5). They contain arsenic in amounts of about 12.2 μg/L and 21.0 μg/L and very high mineralization (1,424 mg/L and 4,568 mg/L), high contents of chlorides (192 mg/L and 693 mg/L), bicarbonates (770 mg/L and 2,502 mg/L), barium (2.8 mg/L and 11.3 mg/L), potassium (13.0 mg/L and 33.3 mg/L), lithium (0.6 mg/L and 1.9 mg/L) and sodium (407 mg/L and 1,220 mg/L; Tab. 4).

What is noteworthy is the relatively high content of strontium in water, ranging from 86 μg/L to 2,370 μg/L (Tab. 5). This metal occurs in concentrations above the detection limit generally only in places where groundwater outflows occur. The strong positive correlations with arsenic, barium, lithium and bicarbonates, and inverse correlations with sulphates, calcium and magnesium are visible which can indicate the geological genesis of this element.

Table 5
The concentration of the elements in water from the Bystre Thrust-Sheet of the potential use possibilities for health resort purposes (max. values in bold)

Element	Unit	"Anna" Spring (R4)	Rabe-1 borehole (R5)	Bystre 1 borehole "Danuta" Spring (J10)	"Karolina" Spring (M2)	Spring near Roztoki Dolne (M3)
Arsenic	µg/L	12.21	21.00	**378.72**	60.15	105.92
Bicarbonates	mg/L	769.50	**2,502.00**	455.28	924.30	1,040.70
Chlorides		191.73	**692.70**	14.73	88.08	138.80
Fluorides		1.05	no data	**3.09**	2.32	no data
Sodium		407.41	**1,220.00**	122.28	346.33	499.88
Potassium		12.96	**33.27**	9.88	5.59	7.14
Lithium		0.61	**1.86**	0.26	0.30	0.44
Strontium	µg/L	667.89	**2,370.00**	882.09	0.66	0.65
Barium	mg/L	2.81	**11.27**	1.02	1.31	0.84
TDS		1,424.17	**4,568.06**	1,023.57	1,457.51	1,817.49

Based on the comparison of arsenic content in subsequent years (2023 and 2024), it was found that they change to a different level, although usually only to a small extent (Fig. 9, Tab. 5). Similar results of arsenic content variation in water from the "Anna" Spring (our R4 point) were obtained in research by Łach & Pasztyła (2013). They found arsenic content ranging from 15 µg/L to 20 µg/L in 2010–2014. This proves that the concentration of this metalloid in water is quite stable and gives good prospects for using water for health resort purposes.

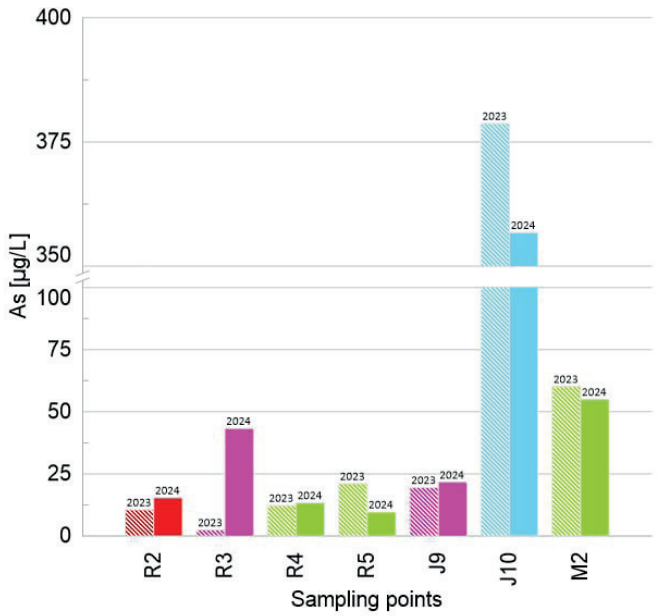

Fig. 9. *Changes in arsenic content in water from the Bystre Thrust-Sheet (points location in Fig. 2 and Tab. 1): in red (R2) – sample from standing water; in pink (R3 and J9) – from streams, in green (R4, R5 and M2) – from springs; in blue (J10) – from borehole*

SUMMARY AND CONCLUSIONS

The analysis of the results obtained in the work allowed for the following conclusions to be drawn:

1. Relatively high concentrations of arsenic only appeared in springs and boreholes. In flowing waters, these concentrations quickly decreased due to either dilution or precipitation and binding to the solid phase.
2. The presence of arsenic-containing water confined to the Bystre Thrust-Sheet area reveals a strong connection between arsenic concentrations in water, arsenic mineralization, and tectonic processes.
3. The conditions prevailing in waters, which are mainly high pH, favour the immobilization of metals in sediments and suspended matter. The lower concentrations of arsenic in flowing waters may be attributed to the strongly calcareous nature of the Cieszyn beds which act as a natural barrier, limiting the migration of arsenic beyond the Bystre Thrust-Sheet.
4. In waters associated with the weathering zone of freshly exposed rocks where realgar-mineralized zones occur, the content of arsenic is not high compared to other places due to the precipitation of arsenic compounds at high pH and sulphur ion content in water.
5. The most probable genesis of arsenic in waters is the dissolution of arsenic minerals occurring in intensively mineralized zones of the Bystre Thrust-Sheet.
6. The presence of arsenic in spring water in areas where mineralization has not been recorded at the surface suggests that arsenic mineralization may occur at greater depths. This proves that the extent of mineralization is much greater than indicated by cartographic studies. The presence of groundwater of the ionic type HCO_3-Na or HCO_3-Cl-Na, in which the highest As content was detected, may indirectly point to the presence of mineralization zones.
7. Groundwater in the Bystre Thrust-Sheet area have a chemical composition that is very favourable in terms of health resorts but when considering water use for health purposes, it is necessary to monitor its arsenic content.

In conclusion, the Bystre Thrust-Sheet area contains groundwater with significant health potential – it has a high degree of mineralization and contains many valuable microelements, including arsenic. However, in some sources, there were above-standard contents of this metalloid detected. Therefore, it is extremely important to ensure the safe use of these waters for therapeutic purposes by carefully managing arsenic levels.

The case described in this paper has universal applications because there are similar places in the world where it is worth using valuable mineral waters, taking into account the need to monitor the concentration of components that may cause toxic effects on humans.

The study was supported financially by AGH University of Krakow in Poland ("Detailed study of the structural framework of the Bystre Thrust-Sheet in the area of geochemical anomalies to identify potential lithium deposits in the Outer Carpathians", IDUB no. 5859 and no. 16.16.140.315).

We would like to thank the members of the AGH UST Geological and Computer Cartography Student Scientific Group "Azymut": R. Szczęch, A. Saczka, M. Pawlak, K. Kucharz, M. Esmund, and Z. Ziarek. We also extend our gratitude to the academic staff of the Faculty of Geology, Geophysics, and Environmental Protection at AGH University of Science and Technology in Krakow, as well as to Professor Marek Nieć and Professor Antoni Tokarski for their invaluable academic support and Gabriel Rączkowski for his support with statistical methods.

We would like to thank the reviewers for their comments which allowed us to improve the quality of the article.

REFERENCES

Alekin O.A., 1970. *Osnovy gidrokhimii* (*Principles of Hydrochemistry*). Gidrometeorologicheskoye Izdatel'stvo, Leningrad [Алекин О.А., 1970. Основы гидрохимии. Гидрометеорологическое Издательство, Ленинград].

Aleksander-Kwaterczak U. & Plenzler D., 2019. Contamination of small urban watercourses on the example of a stream in Krakow (Poland). *Environmental Earth Sciences*, 78, 530. https://doi.org/10.1007/s12665-019-8509-4.

Argos M., Kalra T., Rathouz P.J., Chen Y., Pierce B., Parvez F., Islam T., Ahmed A., Rakibuz-Zaman M., Hasan R., Sarwar G., Slavkovich V., van Geen A., Graziano J. & Ahsan H., 2010. Arsenic exposure from drinking water, and all-cause and chronic-disease mortalities in Bangladesh (HEALS): a prospective cohort study. *The Lancet*, 376(9737), 252–258. https://doi.org/10.1016/S0140-6736(10)60481-3.

Assis I.R., Dias L.E., Ribeiro E.S. Jr., Abrahão W.A.P., Vargas de Mello J.W. & Veloso R.W., 2012. Induction of a geochemical barrier for As, Fe and S immobilization in a sulfide substrate. *Revista Brasileira de Ciência do Solo*, 32, 671–679. https://doi.org/10.1590/S0100-06832012000200036.

Bartram J. & Balance R. (eds.), 1996. *Water quality monitoring – a practical guide to the design and implementation of freshwater quality studies and monitoring programmes*. UNEP/WHO.

Bhattacharjee P., Chatterjee D., Singh K.K. & Giri A.K., 2013. Systems biology approaches to evaluate arsenic toxicity and carcinogenicity: An overview. *International Journal of Hygiene and Environmental Health*, 216(5), 574–586. https://doi.org/10.1016/j.ijheh.2012.12.008.

Bissen M. & Frimmel F.H., 2003. Arsenic – a review. Part I: Occurrence, toxicity, speciation, mobility. *Acta Hydrochimica et Hydrobiologica*, 31(1), 9–18. https://doi.org/10.1002/aheh.200390025.

Bojakowska I. & Borucki J., 1992. Anomalie arsenowe koło Baligrodu i Nowego Łupkowa (Karpaty). *Kwartalnik Geologiczny*, 36(4), 469–480.

Borek L., 2024. The impact of the geographical environment on the hydromorphological conditions of watercourses in southern Poland. *Geology, Geophysics and Environment*, 50(1), 93–112. https://doi.org/10.7494/geol.2024.50.1.93.

Bowell R., Alpers Ch., Jamieson H., Nordstrom D.K. & Majzlan J., 2014. The environmental geochemistry of arsenic: An overview. [in:] Bowell R., Alpers C., Jamieson H., Nordstrom K. & Majzlan J. (eds.), *Arsenic: Environmental Geochemistry, Mineralogy and Microbiology*. De Gruyter, Berlin–Boston, 1–16. https://doi.org/10.1515/9781614517979.1.

Boyd C.E., 2015. *Water Quality: An Introduction*. Springer Cham. https://doi.org/10.1007/978-3-319-17446-4.

Campbell K.M. & Nordstrom D.K., 2014. Arsenic speciation and sorption in natural environments. [in:] Bowell R., Alpers C., Jamieson H., Nordstrom K. & Majzlan J. (eds.), *Arsenic: Environmental Geochemistry, Mineralogy and Microbiology*. De Gruyter, Berlin–Boston, 185–216. https://doi.org/10.2138/rmg.2014.79.3.

Ciszewski D. & Aleksander-Kwaterczak U., 2020. Metal mobility in a mine-affected floodplain. *Minerals*, 10(9), 814. https://doi.org/10.3390/min10090814.

Chaudhary M.M., Hussain S., Du C., Conway B.R. & Ghori M.U., 2024. Arsenic in water: understanding the chemistry, health implications, quantification and removal strategies. *ChemEngineering*, 8(4), 78. https://doi.org/10.3390/chemengineering8040078.

Chung J.Y., Yu S.-D. & Hong Y.S., 2014. Environmental source of arsenic exposure. *Journal of Preventive Medicine and Public Health*, 47(5), 253–257. https://doi.org/10.3961/jpmph.14.036.

Cullen W.R. & Reimer K.J., 1989. Arsenic speciation in the environment. *Chemical Reviews*, 89, 713–764. https://doi.org/10.1021/cr00094a002.

De A. & Roy N., 2023. Consequences of arsenic in the environment. [in:] Huq S.M.I. (ed.), *Arsenic in the Environment – Sources, Impacts and Remedies*. IntechOpen. http://doi.org/10.5772/intechopen.1001476.

Drahota P., Mikutta C., Falteisek L., Duchoslav V. & Klementová M., 2017. Biologically induced formation of realgar deposits in soil. *Geochimica et Cosmochimica Acta*, 218, 237–256. https://doi.org/10.1016/j.gca.2017.09.023.

Fatoki J.O. & Badmus J.A., 2022. Arsenic as an environmental and human health antagonist: A review of its toxicity and disease initiation. *Journal of Hazardous Materials Advances*, 5, 100052. https://doi.org/10.1016/j.hazadv.2022.100052.

Frohne T., Rinklebe J., Diaz-Bone R.A. & Du Laing G., 2011. Controlled variation of redox conditions in a floodplain soil: Impact on metal mobilization and biomethylation of arsenic and antimony. *Geoderma*, 160(3–4), 414–424.

Guven D.E. & Akinci G., 2013. Effect of sediment size on bioleaching of heavy metals from contaminated sediments of Izmir Inner Bay. *Journal of Environmental Sciences*, 25(9), 1784–1794. https://doi.org/10.1016/S1001-0742(12)60198-3.

Hall A.H., 2002. Chronic arsenic poisoning. *Toxicology Letters*, 128(1–3), 69–72. https://doi.org/10.1016/S0378-4274(01)00534-3.

Hiller E., Lalinská B., Chovan M., Jurkovič L., Klimko T., Jankulár M., Hovorič R., Šottník P., Fľaková R., Ženišová Z. & Ondrejková I. 2012. Arsenic and antimony contamination of waters, stream sediments and soils in the vicinity of abandoned antimony mines in the Western Carpathians, Slovakia. *Applied Geochemistry*, 27(3), 598–614. https://doi.org/10.1016/j.apgeochem.2011.12.005.

Hubaux R., Becker-Santos D.D., Enfield K.S., Lam S., Lam W.L. & Martinez V.D., 2012. Arsenic, asbestos and radon: emerging players in lung tumorigenesis. *Environmental Health*, 11, 89. https://doi.org/10.1186/1476-069X-11-89.

Jankowski L., 2015. *Nowe spojrzenie na budowę geologiczną Karpat: ujęcie dyskusyjne*. Instytut Nafty i Gazu – Państwowy Instytut Badawczy, Kraków.

Jankowski L. & Jarmołowicz-Szulc K., 2009. Particular tectonic zones (the mélange zones) as potential and significant paths for fluid migration and mineral formation. *Mineralogical Review*, 59(1), 31–44.

Jankowski L. & Ślączka A., 2000. *Szczegółowa mapa geologiczna Polski w skali 1:50 000: arkusz Jabłonki*. Ministerstwo Środowiska, Warszawa.

Jankowski L. & Ślączka A., 2014. *Objaśnienia do Szczegółowej Mapy Geologicznej Polski w skali 1:50 000: arkusz Jabłonki*. Państwowy Instytut Geologiczny – Ministerstwo Środowiska, Warszawa.

Jarmołowicz-Szulc K. & Jankowski L., 2021. Interpretation of mineralization in the Western Carpathians (Polish segment) – A tectonic mélange approach. *Minerals*, 11(11), 1171. https://doi.org/10.3390/min11111171.

Jarmołowicz-Szulc K., Karwowski Ł. & Marynowski L., 2012. Fluid circulation and formation of minerals and bitumen in the sedimentary rocks of the Outer Carpathians – based on studies on the quartz-calcite-organic matter association. *Marine and Petroleum Geology*, 32(1), 138–158. https://doi.org/10.1016/j.marpetgeo.2011.11.010.

Jarmołowicz-Szulc K., Kleczyński P., Kozłowski A., Gąsienica A. & Giro L., 2023. Przejawy mineralizacji w odniesieniu do procesów geotektonicznych w Karpatach fliszowych – nowe doniesienia. *Przegląd Geologiczny*, 71(4), 188–196. https://doi.org/10.7306/2023.13.

Jarmołowicz-Szulc K., Kleczyński P., Kozłowski A. & Gąsienica A., 2024. Genetic relationship of minerals to fluid circulation in the Polish Carpathians – the Bystre Slice case study. *Geological Quarterly*, 68(11), 1–16. https://doi.org/10.7306/gq.1740.

Kamieński M., 1937. O minerałach arsenowych z fliszu karpackiego okolicy Leska. *Archiwum Mineralogiczne*, 13, 1–8.

Kita-Badak M., 1970. W sprawie mineralizacji arsenowej w okolicy Baligrodu. *Geological Quarterly*, 15(1), 155–160.

Komorowicz I. & Barałkiewicz D., 2016. Determination of total arsenic and arsenic species in drinking water, surface water, wastewater, and snow from Wielkopolska, Kujawy-Pomerania, and Lower Silesia provinces, Poland. *Environmental Monitoring and Assessment*, 188(9), 504. https://doi.org/10.1007/s10661-016-5477-y.

Kucharič Ľ., Bezák V., Kubeš P., Vozár J. & Konečný V., 2012. New magnetic anomalies of the Outer Carpathians in NE Slovakia and their relationship to the Carpathian Conductivity Zone. *Geological Quarterly*, 57, 123–134.

Litwin I., Lis P. & Maciaszczyk-Dziubińska E., 2009. Dwie twarze arsenu. *Kosmos*, 58(1–2), 187–198.

Lu P. & Zhu C., 2011. Arsenic Eh–pH diagrams at 25°C and 1 bar. *Environmental Earth Sciences*, 62, 1673–1683. https://doi.org/10.1007/s12665-010-0652-x.

Łach A. & Pasztyła G., 2013. Unikalne wody litowo-arsenowe w Rabe. *LAB*, 18(6), 6–10.

Malata T., Marciniec P. & Starkel L., 1997. *Szczegółowa Mapa Geologiczna Polski 1:50 000: arkusz Lesko*. Ministerstwo Środowiska, Warszawa.

Mastella L., 1995. *Mapa tektoniczna jednostki przeddukielskiej (między Roztokami Dolnymi a Ustrzykami Górnymi).* Archiwum Instytutu Geologii Podstawowej, UW, Warszawa.

Moore J.N., Ficklin W.H. & Johns C., 1988. Partitioning of arsenic and metals in reducing sulfidic sediments. *Environmental Science & Technology*, 22(4), 432–437. https://doi.org/10.1021/es00169a011.

Newman D.K., Ahmann D. & Morel F.M.M., 1998. A brief review of microbial arsenate respiration. *Geomicrobiology Journal*, 15(4), 255–268. https://doi.org/10.1080/01490459809378082.

Nieć M., Lenik P. & Radwanek-Bąk B., 2016. Szkic metalogenii polskich Karpat – modele i możliwości występowania złóż rud. *Biuletyn Państwowego Instytutu Geologicznego*, 467, 9–40.

Organ M., 2021. "The boundary of the world" – the beginnings of tourism in the Bieszczady Mountains in the 19th century. *Galicja: Studia i Materiały*, 7, 107–138, https://doi.org/10.15584/galisim.2021.7.6.

Ostrowicki B., 1958. Nowe minerały kruszcowe w okolicy Baligrodu. *Kwartalnik Geologiczny*, 2(4), 644–653.

Oszczypko N., Ślączka A. & Żytko K., 2008. Regionalizacja tektoniczna Polski – Karpaty zewnętrzne i zapadlisko przedkarpackie. *Przegląd Geologiczny*, 56(10), 927–935.

Peng J.-f., Song Y.-h., Yuan P., Cui X.-y. & Qiu G.-l., 2009. The remediation of heavy metals contaminated sediment. *Journal of Hazardous Materials*, 161(2–3), 633–640. https://doi.org/10.1016/j.jhazmat.2008.04.061.

Peszat C., Bromowicz J. & Buczek-Pułka M., 1985. Perspektywy dokumentowania złóż i racjonalnego wykorzystania piaskowców województwa krośnieńskiego. *Zeszyty Naukowe AGH*, *Geologia*, 11(4), 5–102.

PN-ISO 9297:1994. Jakość wody – Oznaczanie chlorków – Metoda miareczkowania azotanem srebra w obecności chromianu jako wskaźnika (Metoda Mohra).

PN-EN ISO 9963-1:2001. Jakość wody – Oznaczanie zasadowości – Część 1: Oznaczanie zasadowości ogólnej i zasadowości wobec fenoloftaleiny.

PN-EN ISO 17294-1:2007. Water quality – application of mass spectrometry with inductively coupled plasma (ICP-MS).

PN-EN ISO 11885:2009. Water quality – determination of selected elements by inductively coupled plasma optical emission spectrometry (ICP-OES).

PN-EN ISO 5667-3:2024. Water quality – Sampling – Part 3: Preservation and handling of water samples.

Rahman M.M., Naidu R. & Bhattacharya P., 2009. Arsenic contamination in groundwater in the Southeast Asia region. *Environmental Geochemistry and Health*, 31, 9–21. https://doi.org/10.1007/s10653-008-9233-2.

Rajchel L., 2012. *Szczawy i wody kwasowęglowe Karpat polskich*. Wydawnictwa AGH, Kraków.

Rajchel L., Rajchel J. & Wołowski K., 2002. Microorganisms in selected sulphuric springs of the Polish Carpathians. *Geological Quarterly*, 46(2), 189–198.

Ravenscroft P., Brammer H. & Richards K., 2009. *Arsenic Pollution: A Global Synthesis*. Wiley-Blackwell, Chichester.

Rozporządzenie Ministra Infrastruktury z dnia 25 czerwca 2021 r. w sprawie klasyfikacji stanu ekologicznego, potencjału ekologicznego i stanu chemicznego oraz sposobu klasyfikacji stanu jednolitych części wód powierzchniowych, a także środowiskowych norm jakości dla substancji priorytetowych. Dz.U. 2021 poz. 1475 [*Minister of Infrastructure regulation valid from 25 June 2021, on the classification of the ecological status, ecological potential and chemical status of surface water bodies, and environmental quality standards for priority substances*. Journal of Laws of 2021 item 1475]. https://isap.sejm.gov.pl/isap.nsf/DocDetails.xsp?id=WDU20210001475.

Rubinkiewicz J., 1998. Rozwój spękań ciosowych w płaszczowinie śląskiej w okolicach Baligrodu (Bieszczady Zachodnie – Karpaty zewnętrzne. *Przegląd Geologiczny*, 46(9/1), 820–826.

Rubinkiewicz J., 2007. Fold-thrust-belt geometry and detailed structural evolution of the Silesian nappe–eastern part of the Polish Outer Carpathians (Bieszczady Mts.). *Acta Geologica Polonica*, 57(4), 479–508.

Rybak B., 2000. Związek mineralizacji kruszcowej z tektoniką łuski Bystrego (Bieszczady, Karpaty zewnętrzne). *Przegląd Geologiczny*, 48(11), 1023–1029.

Sajdak M., Siwek J.P., Bojarczuk A. & Żelazny M., 2018. Hydrological and chemical water regime in the catchments of Bystra and Sucha Woda, in the Tatra National Park. *Acta Scientiarum Polonorum: Formatio Circumiectus*, 17(3), 161–173.

Shapiro S.S. & Wilk M.B., 1965. An Analysis of Variance Test for Normality (Complete Samples). *Biometrika*, 52(3–4), 591–611. https://doi.org/10.1093/biomet/52.3-4.591.

Shomar B.H., Müller G. & Yahya A., 2005. Seasonal variations of chemical composition of water and bottom sediments in the wetland of Wadi Gaza, Gaza Strip. *Wetlands Ecology and Management*, 13(4), 419–431. https://doi.org/10.1007/s11273-004-0412-3.

Smedley P.L. & Kinniburgh D.G., 2002. A review of the source, behavior and distribution of arsenic in natural waters. *Applied Geochemistry*, 17, 517–568. https://doi.org/10.1016/S0883-2927(02)00018-5.

Solon J., Borzyszkowski J., Bidłasik M., Richling A., Badora K., Balon J. et al., 2018. Physico-geographical mesoregions of Poland: Verification and adjustment of boundaries on the basis of contemporary spatial data. *Geographia Polonica*, 91(2), 143–170. https://doi.org/10.7163/GPol.0115.

Spearman C., 1904. The proof and measurement of association between two things. *The American Journal of Psychology*, 15(1), 72–101. https://doi.org/10.2307/1412159.

Ślączka A., 1958. O pozycji okruszcowania w okolicy Baligrodu. *Kwartalnik Geologiczny*, 2(4), 637–643.

Świdziński H., 1958. *Mapa geologiczna Karpat polskich: Część wschodnia*. Instytut Geologiczny, Warszawa.

Uddin M.M., Harun-Ar-Rashid A.K.M., Hossain S.M., Hafiz M.A., Nahar K. & Mubin S.H., 2006. Slow arsenic poisoning of the contaminated groundwater users. *International Journal of Environmental Science and Technology*, 3(4), 447–453. https://doi.org/10.1007/BF03325954.

Veloso R.W., Vargas de Mello J.W., Abrahão W.A.P. & Glasauer S., 2019. Seasonal impacts on arsenic mobility and geochemistry in streams surrounding a gold mineralization area, Paracatu, Brazil. *Applied Geochemistry*, 109. https://doi.org/10.1016/j.apgeochem.2019.104390.

WHO (World Health Organization), 2022. *Guidelines for drinking-water quality: Fourth edition incorporating the first and second addenda*. https://iris.who.int/bitstream/handle/10665/352532/9789240045064-eng.pdf?sequence=1.

Wieser T., 1994. Pojurajskie przejawy mineralizacji a procesy geotektoniczne w Karpatach Fliszowych Polski i obszarów ościennych. *Prace Specjalne Polskiego Towarzystwa Mineralogicznego*, 5, 50–51.

Wojciechowski A., 2003. Wystąpienia rtęci i złota w rejonie Baligrodu oraz Szczawnicy (polska część Karpat). *Przegląd Geologiczny*, 51(2), 131–138.

Zhang C., Yu Z.-g., Zeng G.-m., Jiang M., Yang Z.-z., Cui F., Zhu M.-y., Shen L.-g., & Hu L., 2014. Effects of sediment geochemical properties on heavy metal bioavailability. *Environment International*, 73, 270–281. https://doi.org/10.1016/j.envint.2014.08.010.